Lifetimes of noisy repellors

Holger Faisst and Bruno Eckhardt
Fachbereich Physik, Philipps-Universität Marburg, D-35032 Marburg, Germany
(Received 11 March 2003; published 22 August 2003)

We study the effects of additive noise on the lifetimes of chaotic repellors. Using first-order perturbation theory, we argue that noise will increase the lifetime if the escape holes lie in regions where the unperturbed density is higher than that in the immediate vicinity and that it decreases if the density is lower. Numerical experiments support the qualitative conclusions also beyond perturbation theory.

DOI: 10.1103/PhysRevE.68.026215 PACS number(s): 05.45.Ac, 05.45.Df, 05.40.Ca

I. INTRODUCTION

Noise can affect the behavior of dynamical systems in many ways. It can induce transitions between otherwise disconnected regions (Kramers' theory, [1]), it changes the scaling near bifurcations [2], it gives rise to stochastic resonance [3], and it can even change repellors into attractors [4]. Some time ago, Franaszek [5] studied the effects of additive noise on repellors [6] and found that in some cases it stabilized the dynamics, i.e., increased the lifetimes. He studied this behavior near crises and bifurcations in the dynamics, but the reasons for the effects on the dynamics remained unclear. We here want to approach the problem from the side of the attractor which then is perturbed to become a chaotic repellor. We will investigate the relation between the noise effects and a nonuniform density in the attractor.

The hypothesis we want to test runs as follows: opening up the attractor into a repellor is achieved by punching holes into the support of the attractor. Additive noise can push trajectories that would barely miss the holes into escape, but can also save trajectories that would escape in the unperturbed situation. Whether the lifetime increases or decreases then depends on which process is more likely; for a uniform density, noise will kick out as many trajectories as it saves, so one cannot expect any effect. If the unperturbed density in the hole region is higher than that in the immediate vicinity, more points will be saved than kicked out, and the lifetime should increase. If the unperturbed density in the hole region is lower, more trajectories will escape and the lifetime should be reduced.

In Sec. II, we present the perturbative arguments, followed by numerical experiments in Sec. III and some final remarks in Sec. IV.

II. PERTURBATION THEORY

We start with a d-dimensional map

$$\mathbf{x}_{n+1}=\mathbf{f}(\mathbf{x}_n) \tag{1}$$

that has a chaotic attractor. The associated Frobenius-Perron equation for the evolution of densities $\rho(\mathbf{x})$ is

$$\rho_{n+1}(\mathbf{x})=\int d\mathbf{y}\,\delta(\mathbf{x}-\mathbf{f}(\mathbf{y}))\rho_n(\mathbf{y}) \tag{2}$$

$$=\sum_i \frac{\rho_n(\mathbf{y_i})}{|D\mathbf{f}(\mathbf{y}_i)|}, \tag{3}$$

where $|D\mathbf{f}|$ is the Jacobi determinant and the summation extends over all points $\mathbf{y}_i$ that map into $\mathbf{x}$. Noise can be added as a Gaussian smearing of the propagator, as in a kicked system. The time evolution splits into two parts: the ''kick'' (1), i.e., the application of the deterministic map, and a free diffusive spreading. The free diffusion on the d-dimensional phase space is described by a diffusion kernel K_D that solves the appropriate free diffusion equation with δ-function initial conditions. For instance, for free diffusion in Euclidean space, the Fokker-Planck equation for a density ρ is

$$\dot{\rho}=D\Delta\rho \tag{4}$$

and the diffusion kernel becomes

$$K_D(\mathbf{y},\mathbf{x},t)=\frac{1}{(2\pi Dt)^{d/2}}e^{-(\mathbf{y}-\mathbf{x})^2/2Dt}. \tag{5}$$

The combined evolution of kick and diffusion for some time T is then described by

$$\rho_{n+1}(\mathbf{x})=\int d\mathbf{z}K_D(\mathbf{x},\mathbf{z},T)\int d\mathbf{y}\,\delta(\mathbf{z}-\mathbf{f}(\mathbf{y}))\rho_n(\mathbf{y}) \tag{6}$$

$$=\int d\mathbf{y}K_D(\mathbf{x},\mathbf{f}(\mathbf{y}),T)\rho_n(\mathbf{y}) \tag{7}$$

$$=\int d\mathbf{y}K(\mathbf{x},\mathbf{y})\rho_n(\mathbf{y}). \tag{8}$$

The evolution kernel K in Eq. (8) can be expanded in terms of left $\langle\lambda|$ and right eigenfunctions $|\lambda\rangle$ with eigenvalues λ,

$$K=\sum_\lambda \lambda|\lambda\rangle\langle\lambda|. \tag{9}$$

The existence of an invariant density on the attractor (the Sinai-Ruelle-Bowen measure) implies the presence of an eigenvalue $\lambda=1$ with right eigenvector $|1\rangle$, the invariant den-

sity, and a corresponding left eigenvector $\langle 1| = 1$ because of conservation of probability. Since the kernel K is not self-adjoint, left and right eigenvectors are different. Simple examples show that the left eigenvectors develop fractal features [7]. With noise the finest scale structures are washed out, but higher levels of the fractal hierarchy survive.

In order to turn the attractor into a chaotic repellor, we punch holes into it. In applications the holes appear through crises and other perturbations and appear on many scales. For the purpose of the present analysis, trajectories that enter the holes may be terminated, since their further evolution does not influence the escape rate. Let $\mathcal{O}$ be the domain over which trajectories are taken out and P the elimination projection:

$$P(\mathbf{x},\mathbf{z}) = \delta(\mathbf{x}-\mathbf{z}) \begin{cases} 1, & \mathbf{x} \notin \mathcal{O} \\ p, & \mathbf{x} \in \mathcal{O}. \end{cases} \tag{10}$$

This projection depends on a parameter p that will be useful in tests of the perturbation calculations: Trajectories entering $\mathcal{O}$ continue on with probability p and are taken out with probability $1-p$. For the holes described before, we have to take $p=0$. The full evolution operator can then be written as

$$K_P(\mathbf{x},\mathbf{y}) = \int d\mathbf{z} P(\mathbf{x},\mathbf{z}) K(\mathbf{z},\mathbf{y}) \tag{11}$$

$$= K(\mathbf{x},\mathbf{y}) - \int_{\mathcal{O}} d\mathbf{z} [\, \delta(\mathbf{x},\mathbf{z}) - P(\mathbf{x},\mathbf{z})] K(\mathbf{z},\mathbf{y}) \tag{12}$$

$$= K(\mathbf{x},\mathbf{y}) + \alpha K_1(\mathbf{x},\mathbf{y}). \tag{13}$$

The last equation now has the form of an unperturbed propagator K plus a small perturbation αK_1, where smallness is controlled by the localization in the region $\mathcal{O}$ and the rate $1-p$ with which points are taken out. α is a formal parameter that helps to organize the familiar perturbation expansion for eigenvalues and eigenvectors. The leading order result contains as usual the diagonal matrix element of the perturbation,

$$\lambda \approx \lambda_0 + \alpha \langle \lambda | K_1 | \lambda \rangle. \tag{14}$$

The deviations of the leading eigenvalue from $\lambda_0 = 1$ define a decay rate, $\lambda = \exp(-\gamma)$, where

$$\gamma \approx -\alpha \langle \lambda | K_1 | \lambda \rangle. \tag{15}$$

The systems we study here have piecewise smooth invariant densities and the first-order correction to the decay rate has a regular dependence on the set $\mathcal{O}$ and the extraction rate p. In particular, for the logistic map with holes with $p=0$ that is studied in Ref. [8], expression (15) gives the smooth background. The simulations by Paar and Pavin [8] also indicate strong variations in escape rate near short periodic orbits which are connected to higher orders in perturbation theory and the complicated spatial structures that are characteristic for next to leading eigenvectors [7].

III. PIECEWISE LINEAR MAPS WITH NONCONSTANT INVARIANT DENSITIES

Let us define a family of one-dimensional maps $x_{n+1} = f_c(x_n)$ with a parameter $c \in (0,0.5)$,

$$f_c(x) = \begin{cases} x/c, & 0 < x \leqslant c \\ 1-2(x-c)c/(1-2c), & c < x \leqslant 1/2 \\ c-(2x-1)c/(1-2c), & 1/2 < x \leqslant 1-c \\ 1+(x-1)/c, & 1-c < x \leqslant 1. \end{cases} \tag{16}$$

The invariant density is a solution to the Frobenius-Perron equation

$$\rho_c(x) = \int_0^1 dy\, \delta[x - f_c(y)] \rho_c(y) \tag{17}$$

$$= \sum_{x=f_c(x_i)} \frac{\rho_c(x_i)}{|f_c'(x_i)|}, \tag{18}$$

where the sum is taken over all preimages x_i of x. For Eq. (16), the normalized invariant density is

$$\rho_c(x) = \begin{cases} \dfrac{1}{4c(1-c)}, & 0 < x < c \ \text{ and } \ 1-c < x < 1 \\ \dfrac{1}{2(1-c)}, & c < x < 1-c. \end{cases} \tag{19}$$

The main results do not depend on the specific value of c so that we can fix $c=0.2$ and drop the subscript on f and ρ.

For the eigenvalue and eigenvector analysis, we use a matrix representation of the density evolution operator K. With the help of N characteristic functions ϕ_ν,

$$\phi_\nu(x) = \begin{cases} 1, & (\nu-1)/N < x < \nu/N, \quad \nu = 1, \ldots, N \\ 0, & \text{elsewhere,} \end{cases} \tag{20}$$

densities can be expanded as $\rho = a_\nu \phi_\nu$ (summation implied) and the evolution operator K becomes an $N \times N$ matrix. Densities are mapped according to

$$a_\nu^{(n+1)} = K_{\nu\mu} a_\mu^{(n)}, \tag{21}$$

and the matrix elements $K_{\nu\mu}$ can be calculated from the images of the step functions: in the support of the characteristic function μ, a uniformly distributed ensemble of 5×10^5 points is iterated and the probability to end up in the interval ν is then the matrix element $K_{\nu\mu}$. The typical size of matrices used in the calculations is $N = 3000$.

The lifetimes for the maps with holes can be obtained from the eigenvalues of the evolution operator after projection onto the remaining intervals or directly from integrations of an ensemble of initial conditions. We followed 10^6 randomly selected initial points up to a maximal cutoff lifetime of 10^4 iterations. The lifetime distributions decayed exponentially and the lifetimes estimated from this decay were within less than 1% of the eigenvalues.

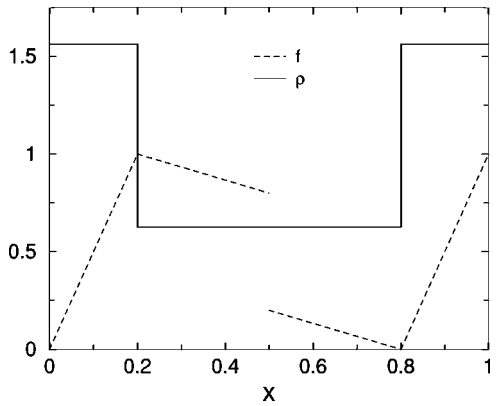

FIG. 1. A graph of map (16) for $c=0.2$ (dashed) and its invariant density ρ (continuous).

A. No holes and no noise

Without noise and without holes, map (16) maps the interval $[0,1]$ into itself. We expect one eigenvalue 1 with the invariant density as right eigenvector (as in Fig. 1), and a left eigenvector that is constant because of conservation of probability. The first two pairs of left and right eigenvectors are shown in Fig. 2. The next to leading eigenvalue is $\lambda_1=-0.6$. Its left eigenvector shows the fractal structures one expects for such maps [7].

B. With holes but without noise

Pairs of holes of size ϵ are added symmetrically at the edges of the invariant density. "Outer" holes at $(c-\epsilon,c)$ and $(1-c,1-c+\epsilon)$ lie within the high density region, "inner" holes at $(c,c+\epsilon)$ and $(1-c-\epsilon,1-c)$ in the low density region.

The perturbation theory from Sec. II predicts a linear variation of escape rate with hole size, so that the ratio of escape rate to hole size should be constant. This is verified in Fig. 3. The numerical values for the escape rate γ agree well

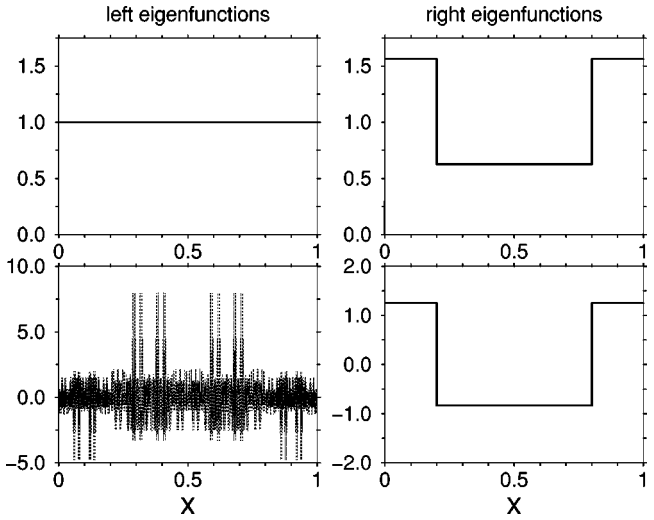

FIG. 2. Eigenfunctions of map without noise and without holes. The upper row corresponds to the leading eigenvalue $\lambda_0=1$ and the lower one to the next to leading eigenvalue $\lambda_1=-0.6$.

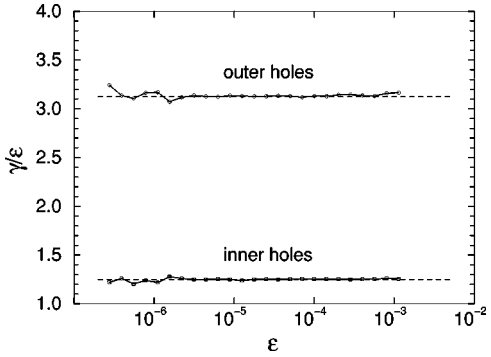

FIG. 3. Escape rate γ divided by the hole size ϵ for map (16) with holes but without noise. The dashed lines at 3.125 and 1.125 mark the values expected within first-order perturbation theory.

with the expected values, sum of hole sizes times undisturbed density at holes, $\gamma_{i,o}=2\epsilon\rho_{i,o}$.

With holes we no longer have conservation of probability, and the left eigenvector to the leading eigenvalue will not be constant. It develops a fractal structure, which already for hole size $\epsilon=10^{-3}$ is difficult to represent numerically. The left eigenstate for the leading eigenvalue $\lambda_0=0.996\,855$ for the map with outer holes is shown in Fig. 4. The largest eigenvalue corresponds to an escape rate $\gamma_o=3.150\times10^{-3}$ in good agreement with the values extracted from Fig. 3.

C. Noisy map without holes

For the map with noise, we add Gaussian distributed random numbers at each time step,

$$x_{n+1}=f(x_n)+\xi_n, \tag{22}$$

where the ξ_n are independent and identically distributed according to

$$p(\xi)=\frac{1}{\sqrt{\pi\sigma^2}}e^{-\xi^2/\sigma^2}, \tag{23}$$

with $\sigma=\sqrt{2Dt}$ the amplitude of the noise. Since it is then possible to leave the interval $[0,1]$, we close the system periodically by mapping points outside the interval back in

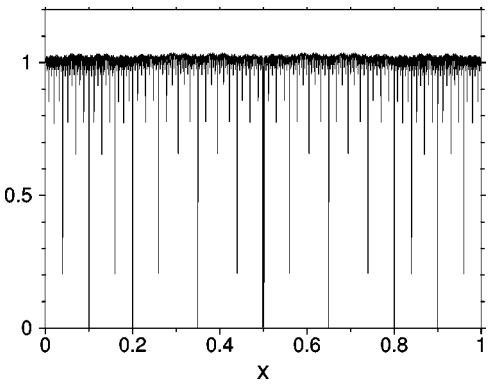

FIG. 4. Left eigenfunction of map with outer holes of size $\epsilon=10^{-3}$ for the leading eigenvalue λ_0. The hierarchy of peaks follows the preimages of the holes.

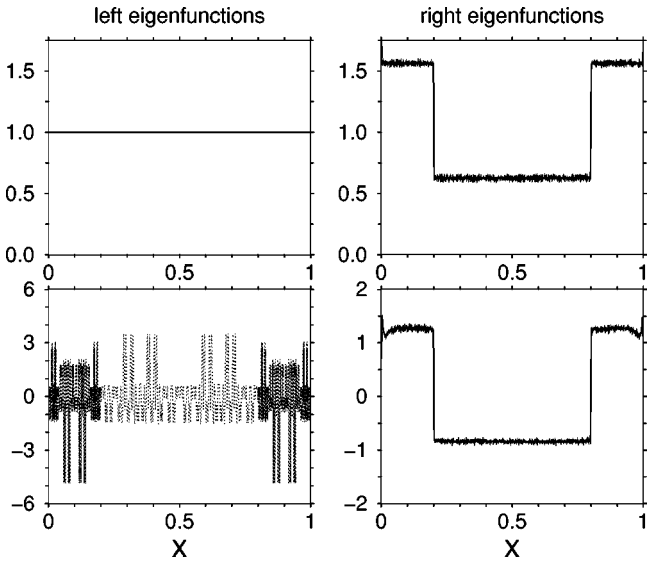

FIG. 5. Eigenfunctions for the noisy map without holes. The noise amplitude is $\sigma=10^{-3}$. The upper row corresponds to the leading eigenvalue $\lambda_0=1$, the lower to the next to leading eigenvalue $\lambda_1=-0.6073$.

using the modulo operation. The case with noise is the more regular one, and if the width of the characteristic function for the hole region is a fraction of the noise level, the vectors converge rather reliably, as a comparison between the results for matrix sizes $N=3000$ and $N=4000$ for noise amplitude 10^{-3} showed.

The eigenfunctions and eigenvalues in the presence of noise of amplitude $\sigma=10^{-3}$ are shown in Fig. 5. The first eigenvalue remains at 1, the first left eigenvector is uniform, but the step in the first right eigenvector is smoothed out. With increasing noise amplitude, this transition region becomes wider, as evidenced by the magnifications in Fig. 6.

D. Noisy map with holes

We finally come to our model for a noisy repellor, the noisy map with holes. Figure 7 shows for holes of size $\epsilon=10^{-3}$ the change in the escape rates as a function of noise amplitude. For outer holes the escape rate decreases, for inner holes it increases, until for a noise amplitude of about

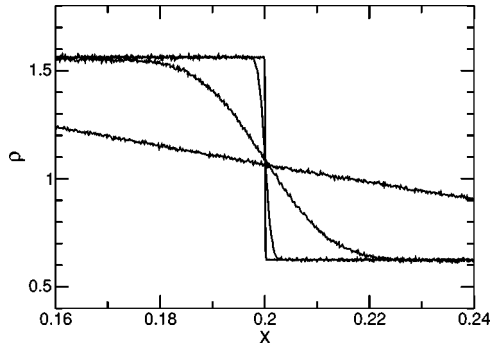

FIG. 6. Magnification of the invariant density for the noisy map without holes. Noise amplitudes are $\sigma=10^{-5}$ (sharpest transition), 10^{-3}, 10^{-2}, and 10^{-1} (widest transition).

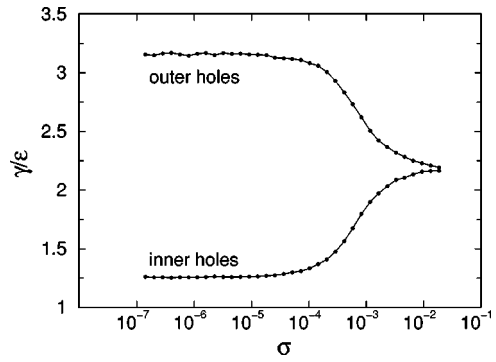

FIG. 7. Escape rate γ divided by the hole size $\epsilon=10^{-3}$ for the noisy map with holes. When the holes are in the high density region (outer holes) the escape rate decreases, and when they are in the low density region (inner holes) it increases. When noise level σ and hole size are comparable, there is no difference between inner and outer hole placements anymore.

10^{-2} they almost coincide. This is exactly what one would expect from the changes in invariant density shown in Fig. 6: the density on the upper level decreases and the one on the lower increases with the corresponding changes in lifetime. If we had not closed the interval to a circle, the loss of trajectories at the end of the intervals would have swamped this effect and the escape rate would have increased monotonically with noise level.

The associated eigenfunctions are shown in Fig. 8 for outer holes of size 10^{-3} together with a noise amplitude 10^{-3}. Compared to the noise free case, structures are smoothed out: for instance, the amplitudes of left eigenfunctions decrease considerably.

E. Failure of perturbation theory

First-order perturbation theory does not always work that well. Consider another map, $x_{n+1}=g(x_n)$ on the interval $[0,1]$ with

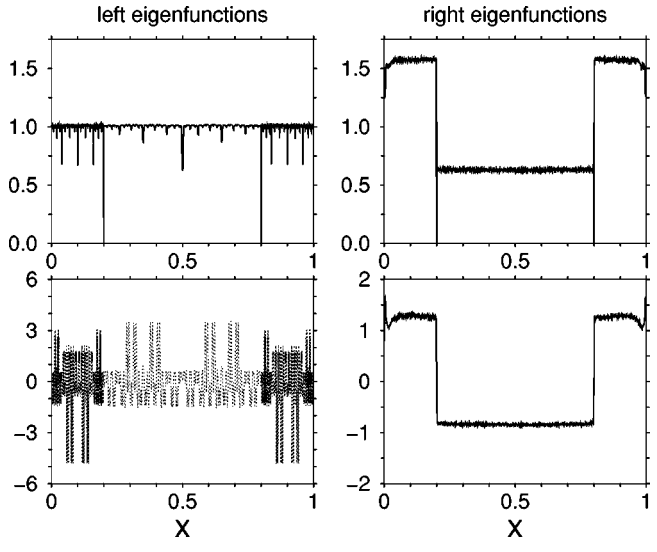

FIG. 8. Eigenfunctions of the map with noise amplitude $\sigma=10^{-3}$ and with outer holes of size $\epsilon=10^{-3}$. The eigenvalues are $\lambda_1=0.997\,45$ for the upper graph and $\lambda_2=-0.611\,38$ for the lower one.

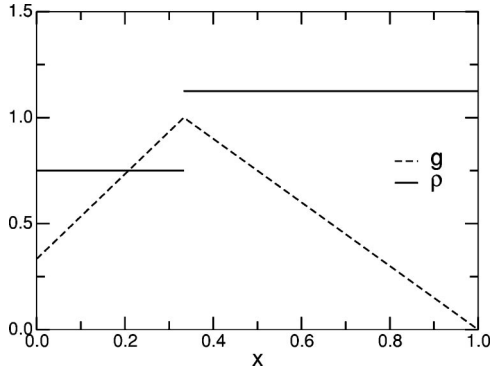

FIG. 9. Map (24) (dashed) and its invariant density (continuous).

$$g(x)=\begin{cases}1/3+2x, & 0<x\leqslant 1/3\\ 3(1-x)/2, & 1/3<x\leqslant 1.\end{cases} \tag{24}$$

Its invariant density is (Fig. 9)

$$\rho(x)=\begin{cases}3/4, & 0<x\leqslant 1/3\\ 9/8, & 1/3<x\leqslant 1.\end{cases} \tag{25}$$

Eigenfunctions for the two leading eigenvalues are shown in Fig. 10. Again we take a left hole at $[1/3-\epsilon,1/3]$ in the low density region and a right hole at $[1/3,1/3+\epsilon]$ in the high density region. First-order perturbation theory predicts the decay rates γ as functions of hole size ϵ to be

$$\gamma_r=\epsilon\rho_r=9/8\epsilon, \tag{26}$$

$$\gamma_l=\epsilon\rho_l=3/4\epsilon. \tag{27}$$

The numerical values extracted from Fig. 11 are

$$\gamma_r=0.87\epsilon, \tag{28}$$

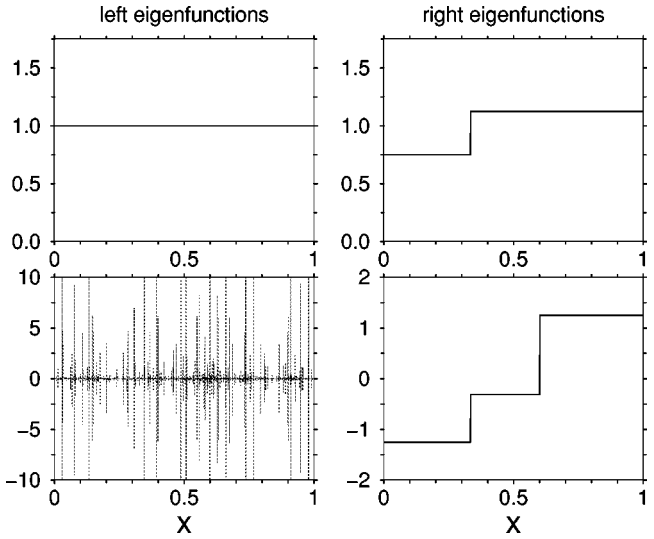

FIG. 10. Eigenfunctions for the leading eigenvalue $\lambda_0=1$ and the next to leading eigenvalue $\lambda_1=-2/3$ for map (24).

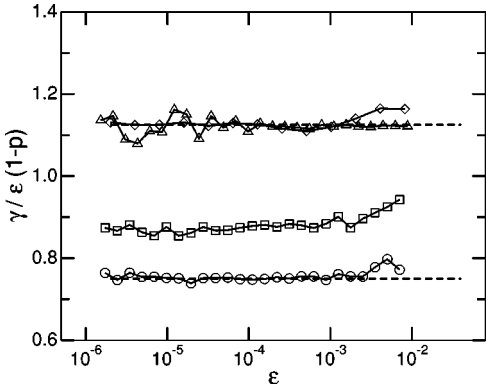

FIG. 11. Escape rates γ divided by hole size ϵ and by $(1-p)$ for map (24) vs hole size for two placements of the hole and two extraction rates p. The dashed horizontal lines mark the theoretical values 9/8 and 3/4. For the left hole, the escape rate is in agreement with perturbation theory (circles, for $p=0$). For the opening to the right at $p=0$ (squares), the prefactor does not agree with perturbation theory. For $p=0.99$, the values move up to the first-order perturbation theory result (triangles). If the position of the opening is moved away from the critical point $x=1/3$, e.g., to the interval $[0.35,0.35+\epsilon]$, then the perturbative result is also obtained for $p=0$ (diamonds).

$$\gamma_l=0.75\epsilon. \tag{29}$$

In agreement with perturbation theory, the escape rate is proportional to the hole size. The prefactors from the two calculations agree for the left hole in the low, but disagree for the right one in the high density region. The deviation becomes smaller when the holes are partially closed, i.e., the parameter p in Eq. (10) is set to 0.99. Then the perturbative and numerical escape rates are in better agreement. This failure of the perturbative estimate seems to be closely connected with the presence of a periodic orbit on the border of the interval. If the opening is shifted to slightly larger values, then the slope agrees again with the perturbative results.

IV. FINAL REMARKS

Within the simple models studied here, the hypothesis that the variation of lifetimes can be related to inhomogeneities in the invariant density of the unperturbed attractor could be confirmed. Such inhomogeneities are most pronounced near bifurcations and crises [9], as in the work of Franaszek [5]. The placement of holes from the outside is less artificial than it may seem. In the case of riddling bifurcations [10], line attractors are broken up by holes that appear near periodic points that are no longer transversally stable, and both position and widths can be controlled externally. Thus, the observations discussed here have some bearing on the effects of noise on the lifetimes in riddled attractors.

ACKNOWLEDGMENT

Support from the Deutsche Forschungsgemeinschaft is gratefully acknowledged.

[1] P. Hänggi, P. Talkner, and M. Borkovec, Rev. Mod. Phys. **62**, 251 (1990).
[2] B. Shraiman, C.E. Wayne, and P.C. Martin, Phys. Rev. Lett. **46**, 935 (1981).
[3] L. Gammaitoni, P. Hänggi, P. Jung, and F. Marchesoni, Rev. Mod. Phys. **70**, 223 (1998).
[4] L. Arnold, H. Crauel, and V. Wihstutz, SIAM J. Control Optim. **21**, 451 (1983); H. Crauel, Arch. Math. **75**, 472 (2000).
[5] M. Franaszek, Phys. Rev. A **44**, 4065 (1991); M. Franaszek and L. Fronzoni, Phys. Rev. E **49**, 3888 (1994).
[6] T. Tél, in *Directions in Chaos*, edited by Hao Bai-Lin (World Scientific, Singapore, 1990), Vol. 3, p. 149.
[7] P. Gaspard, I. Claus, T. Gilbert, and J.R. Dorfman, Phys. Rev. Lett. **86**, 1506 (2001); P. Gaspard, *Chaos, Scattering and Statistical Mechanics* (Cambridge University Press, Cambridge, 1998); S. Tasaki and P. Gaspard, J. Stat. Phys. **81**, 935 (1995); P. Gaspard, G. Nicolis, A. Provata, and S. Tasaki, Phys. Rev. E **51**, 74 (1995).
[8] V. Paar and N. Pavin, Phys. Rev. E **55**, 4112 (1997).
[9] C. Grebogi, E. Ott, and J.A. Yorke, Physica D **7**, 181 (1983).
[10] A.S. Pikovsky and P. Grassberger, J. Phys. A **24**, 4587 (1991); E. Ott, J.C. Alexander, I. Kan, J.C. Sommerer, and J.A. Yorke, Physica D **76**, 384 (1994).